

Renormalization and universality of the Hofstadter spectrum

Hans Koch ¹ and Saša Kocić ²

Abstract. We consider a renormalization transformation \mathfrak{R} for skew-product maps of the type that arise in a spectral analysis of the Hofstadter Hamiltonian. Periodic orbits of \mathfrak{R} determine universal constants analogous to the critical exponents in the theory of phase transitions. Restricting to skew-product maps over a circle-rotations by the golden mean, we find several periodic orbits for \mathfrak{R} , and we conjecture that there are infinitely many. Interestingly, all scaling factors that have been determined to high accuracy appear to be algebraically related to the circle-rotation number. We present evidence that these values describe (among other things) local scaling properties of the Hofstadter spectrum.

1. The Hofstadter model

The spectrum of the Hofstadter Hamiltonian [1,2] exhibits local self-similarity and scaling properties. Using renormalization, we argue that the scaling constant are universal, and that many can be computed exactly. Some of our results are rigorous, while others are based on numerical computations and hypotheses that remain to be verified.

The Hofstadter Hamiltonian describes Bloch electrons moving on \mathbb{Z}^2 under the influence of a magnetic flux $2\pi\alpha$ through each unit cell. It is given by

$$H^\alpha = \lambda'(U_\alpha + U_\alpha^*) + \lambda(V_\alpha + V_\alpha^*), \quad U_\alpha V_\alpha U_\alpha^{-1} V_\alpha^{-1} = e^{-2\pi i \alpha}, \quad (1.1)$$

where U_α, V_α are magnetic translations and λ, λ' are positive constants. In the Landau gauge, $(U_\alpha \phi)(n, m) = \phi(n - 1, m)$ and $(V_\alpha \phi)(n, m) = e^{2\pi i n \alpha} \phi(n, m - 1)$.

For rational $\alpha = m/n$ with m and n coprime, the spectrum of H^α consists of n bands (closed intervals), separated by gaps (open intervals), except at energy zero. The width of these bands tend to zero as $n \rightarrow \infty$. Numerically, the gaps are found to stay open as $m/n \rightarrow \alpha$. Another important observation [5] is the following. Consider the integrated density of states $d(\alpha, E) = \langle \delta_0, P_E^\alpha \delta_0 \rangle$, where P_E^α is the spectral projection for H^α associated with the interval $(-\infty, E]$, and where δ_0 is the Kronecker delta at the origin. For each spectral gap there exists an index $k \in \mathbb{Z}$, also known as the Hall conductance, such that

$$d(\alpha, E) \equiv k\alpha \pmod{1}, \quad (1.2)$$

for all energies E in that gap. The gaps are believed to be open for every α . So far this has been proved for Liouville values [16,20] and Diophantine values [18] if $\lambda \ll \lambda'$ or $\lambda' \ll \lambda$.

The spectrum for irrational α is a Cantor set [20] of measure $4|\lambda' - \lambda|$, as was conjectured in [3] and proved later in [9,10]. The generalized eigenfunctions for $\lambda > \lambda'$ are localized in the n -direction and extended in the m -direction; the same holds for $\lambda' > \lambda$, but with m and n exchanged.

The dual Hamiltonian, obtained by interchanging λ and λ' , is unitarily equivalent to H^α . Of particular interest is the self-dual case $\lambda = \lambda'$. The spectrum for this family of

¹ Dept. of Mathematics, The University of Texas at Austin, Austin, TX 78712.

² Dept. of Mathematics, The University of Mississippi, P.O. Box 1848, University, MS 38677-1848.

operators H^α , plotted as points (α, E) in the plane, is known as the Hofstadter butterfly [2]. The positive-energy part is shown in Figure 1 for $\lambda = \lambda' = 1$. To be more precise, the solid regions are the spectral gaps, and the color encodes the gap index k . The largest regions are for $k = 0$ (white) and $k = \pm 1$.

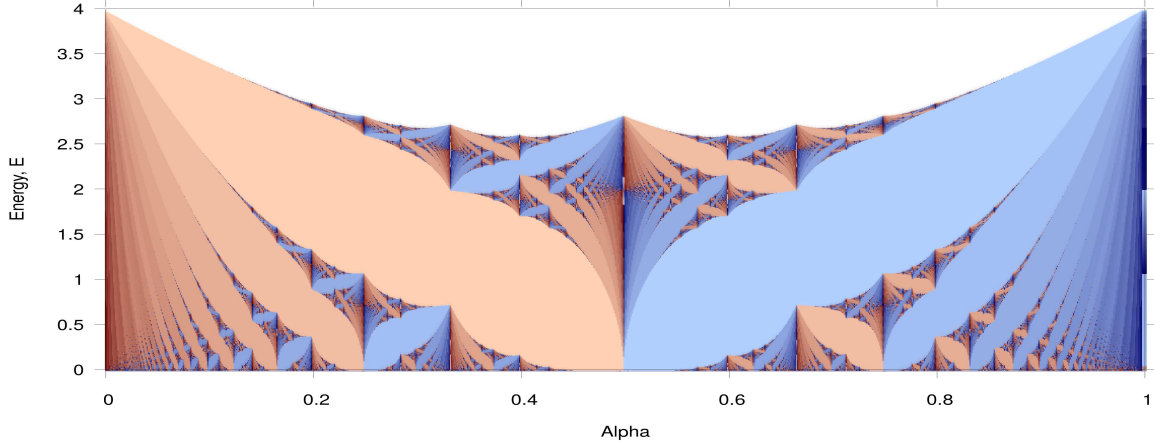


Figure 1. Positive-energy part of the Hofstadter butterfly.

There exists an extensive literature on the topological features of the Hofstadter butterfly and their connection with continued fractions; see e.g. [12,13,15,22] and references therein. In this paper, we are interested mostly in metric properties, especially accumulation phenomena in the energy direction, or for variations in λ . Other scaling properties will be described as well.

To simplify the analysis, we focus mainly on the inverse golden mean $\alpha_* = \frac{1}{2}(\sqrt{5}-1)$. Figure 2 shows successive magnifications of the Hofstadter butterfly near the point $(\alpha_*, 0)$. As will be described below, each magnification step is a composition of three basic steps, and self-similarity occurs with a period $\ell = 6$. Based on high-accuracy computations, we conjecture that the six-step scaling factor μ_1 is the largest root of the polynomial \mathcal{P}_6 given below. Its numerical value is $\mu_1 = 196.29 \dots$

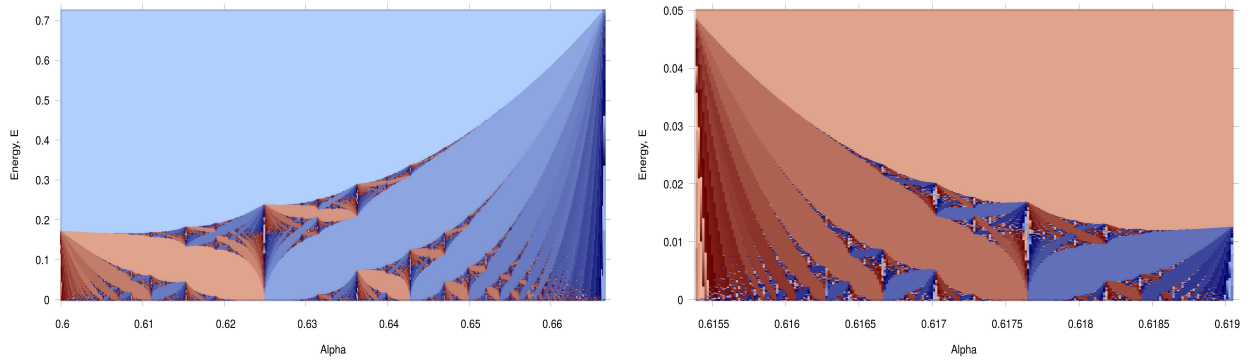


Figure 2. 3-step and 6-step enlargements of the Hofstadter butterfly near $(\alpha_*, 0)$.

Another scaling of the Hofstadter butterfly was described in [23] near the point

(α_*, E_3) , where $E_3 = 2.597\dots$ is the largest value in the spectrum of H^{α_*} . In that case, self-similarity occurs with a period $\ell = 3$, and the three-step scaling factor is $\mu_1 = 30.790\dots$. We conjecture that μ_1 is the largest root of \mathcal{P}_3 , where

$$\begin{aligned}\mathcal{P}_3(z) &= z^4 - 30z^3 - 24z^2 - 10z - 1, \\ \mathcal{P}_6(z) &= z^4 - 196z^3 - 58z^2 - 4z + 1.\end{aligned}\tag{1.3}$$

We note that the product of the two real roots of \mathcal{P}_ℓ is $(-\alpha_*)^{-\ell}$. Their average ζ satisfies $\zeta^2 - 15\zeta - 5 = 0$ in the case $\ell = 3$, and $\zeta^2 - 98\zeta - 19 = 0$ in the case $\ell = 6$. Using these relations, it is easy to write down explicit expressions for the real roots of \mathcal{P}_ℓ . Other scaling points (α_*, E_ℓ) , where we expect similar results, will be described below. But our computations in those cases are not accurate enough to yield a good guess for \mathcal{P}_ℓ .

2. Skew-product maps

The Hamiltonian H^α commutes with the dual magnetic translations, one of which is given by $(\mathcal{U}_\alpha \phi)(n, m) = \phi(n, m - 1)$. So its spectrum can be determined by restricting H^α to generalized eigenfunctions $\phi_\xi(n, m) = e^{-2\pi i m \xi} u_n$ of the translation \mathcal{U}_α . The restricted Hamiltonian \mathcal{H}^α , also known as the almost Mathieu (AM) Hamiltonian, is defined by $(H^\alpha \phi_\xi)(n, m) = e^{-2\pi i m \xi} (\mathcal{H}^\alpha u)_n$ and takes the form of a Schrödinger operator

$$(\mathcal{H}^\alpha u)_n = u_{n-1} + u_{n+1} + V(n\alpha)u_n, \quad n \in \mathbb{Z}, \tag{2.1}$$

with (quasi)periodic potential $V(x) = 2\lambda \cos(2\pi(x + \xi))$. The equation $\mathcal{H}^\alpha u = Eu$ for a generalized eigenvector of \mathcal{H}^α can be written as

$$\begin{bmatrix} u_{n+1} \\ u_n \end{bmatrix} = A(n\alpha) \begin{bmatrix} u_n \\ u_{n-1} \end{bmatrix}, \quad A(x) = \begin{bmatrix} E - V(x) & -1 \\ 1 & 0 \end{bmatrix} \in \text{SL}(2, \mathbb{R}). \tag{2.2}$$

When combined with a rotation $x \mapsto x + \alpha$ of the circle $\mathbb{T} = \mathbb{R}/\mathbb{Z}$, this recursion defines a skew-product map G ,

$$G(x, y) = (x + \alpha, A(x)y), \quad x \in \mathbb{T}, \quad y \in \mathbb{R}^2. \tag{2.3}$$

Two dynamical quantities of interest here are the Lyapunov exponent $L(G)$ and the fibered rotation number $\varrho(G)$. They can be defined as follows. Let \mathcal{G} be a lift of the map $(x, y) \mapsto (x + \alpha, \|A(x)y\|^{-1}A(x)y)$ from $\mathbb{T} \times \mathbb{S}$ to $\mathbb{T} \times \mathbb{R}$, where \mathbb{S} denotes the unit circle $\|y\| = 1$ in \mathbb{R}^2 . Then

$$L(G) = \lim_{n \rightarrow \infty} \frac{1}{n} \log \|(\text{mat } G^n)(x)\|, \quad \varrho(G) = \lim_{n \rightarrow \infty} \frac{1}{2\pi n} \arg \mathcal{G}^n(x, \vartheta). \tag{2.4}$$

Here, $\text{mat } G^n$ denotes the matrix part of G^n , and $\arg(x, \vartheta) = \vartheta$. Assuming that $A : \mathbb{T} \rightarrow \text{SL}(2, \mathbb{R})$ is continuous and α irrational, the limit for $\varrho(G)$ exists, is independent of x and ϑ , independent modulo 1 of the choice of the lift \mathcal{G} , and convergence is uniform. Under the

same assumptions, the limit for $L(G)$ exists and is a.e. constant in x . If G is an AM skew-product for energy E , then the fibered rotation number is related to the density of states via $d(\alpha, E) \equiv -2\varrho(G)$ modulo 1. Furthermore, $L(G) = \max(0, \log |\lambda|)$, if E belongs to the spectrum of \mathcal{H}^α . For proofs of these facts we refer to [4,6,7,19].

Figure 3 depicts two scaling properties of the self-dual AM map G for energy E near the above-mentioned points E_ℓ in the spectrum of $H^{\alpha*}$. The graph on the left shows the logarithm of the Lyapunov exponent $f(E) = L(G)$ as a function of the logarithm of $\epsilon = |E - E_\ell|$, in the case $\ell = 3$. Based on our renormalization analysis described below, we expect that

$$f(E) \simeq C_\pm(\log \epsilon)\epsilon^\tau, \quad \tau = \frac{\ell \log(\alpha_*^{-1})}{\log(\mu_1)}, \quad (2.5)$$

as $E \rightarrow E_\ell$ from below ($-$) or from above ($+$). The functions C_\pm are periodic with period $\log(\mu_1)$, where μ_1 is the largest root of \mathcal{P}_ℓ . The same behavior is observed for $\ell = 6$. In the case $\ell = 3$, the function C_+ is constant, since $H^{\alpha*}$ has no spectrum above E_3 .

The graph in the right part of Figure 3 shows the logarithm of $f(E) = 2|\rho(E) - \rho(E_\ell)|$ versus $\log \epsilon$ in the case $\ell = 6$. Here, $\rho(E)$ denotes the fibered rotation number of the self-dual AM map with energy E . The predicted behavior is again of the form (2.5), both for $\ell = 3$ and $\ell = 6$. The value of τ given by (2.5), as well as the period of C_\pm , match our numerical data at the precision available.

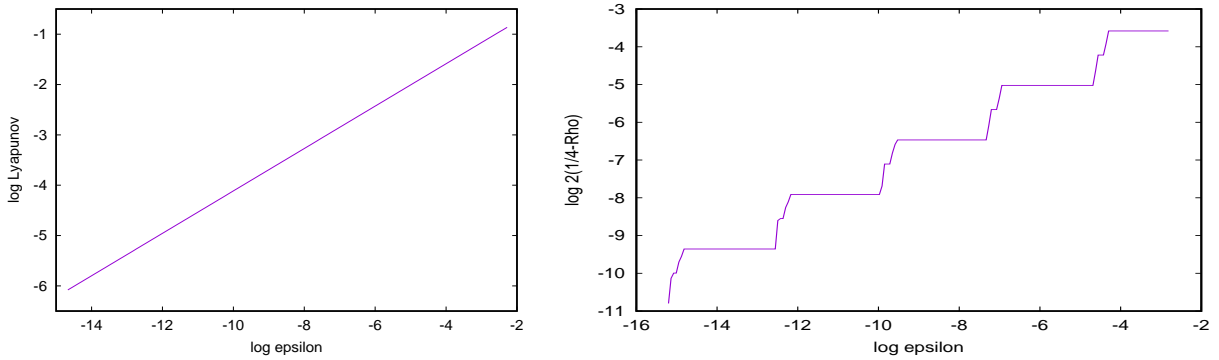


Figure 3. Scaling of L for $E > E_3$ near E_3 (left) and of $1/4 - \varrho$ for small $E > E_6 = 0$ (right).

3. Renormalization

The observation of such asymptotic scaling suggests that a suitable renormalization transformation \mathfrak{R} for skew-product maps has a periodic point P_* of period ℓ , and that μ_1 is the largest eigenvalue of the derivative $D\mathfrak{R}^\ell(P_*)$. Let G be a skew-product map as in (2.3), henceforth abbreviated as $G = (\alpha, A)$. Regard G as a map on $\mathbb{R} \times \mathbb{R}^2$. If G arises from a Schrödinger operator (2.1) with a 1-periodic potential V , then we pair G with a second skew-product map $F = (1, I)$. The 1-periodicity of the matrix function A is expressed by the fact that G commutes with F . As was observed and used in [23], the AM map G with potential $V(x) = 2\lambda \cos(2\pi(x + \xi))$ and $\xi = \alpha/2$ is reversible, in the sense that

$$G^{-1} = S G S, \quad S(x, y) = (-x, S y), \quad S = \begin{bmatrix} 0 & 1 \\ 1 & 0 \end{bmatrix}. \quad (3.1)$$

Thus, we restrict now to pairs $P = (F, G)$ that are reversible, and we choose our renormalization transformation to preserve reversibility, provided that F and G commute. The matrix parts of F and G are always assumed to take values in $\text{SL}(2, \mathbb{R})$. The transformation \mathfrak{R} considered in [23] is given by

$$\mathfrak{R}(P) = (\Lambda_1^{-1} G \Lambda_1, \Lambda_1^{-1} F G^{-1} \Lambda_1), \quad \Lambda_1(x, y) = (\alpha_* x, S e^{\sigma_1 S} y), \quad (3.2)$$

where $\sigma_1 = \sigma_1(P)$ is determined by a suitable normalization condition. We note that this choice of \mathfrak{R} is tailored to the study of skew-product maps $G = (\alpha, A)$ with $\alpha = \alpha_*$. Due to the identity $1 - \alpha_* = \alpha_*^2$, a pair $((1, B), (\alpha_*, A))$ is mapped to a pair $((1, B_1), (\alpha_*, A_1))$. Analogous transformations can be defined for other quadratic irrationals α . Approximate renormalization schemes and limiting cases have been considered earlier in [14, 17].

It is instructive to consider what happens to fibered rotation numbers under renormalization. Let $F = (\beta, B)$ and $G = (\alpha, A)$, with α and β irrational. Assume that A and B are continuous 1-periodic functions on \mathbb{R} , taking values in $\text{SL}(2, \mathbb{R})$. If F and G commute, then $\varrho(FG) \equiv \varrho(F) + \varrho(G)$ modulo 1. This follows e.g. from the uniform convergence [6] of the second limit in (2.4). As a consequence, if $(F_1, G_1) = \mathfrak{R}(F, G)$, then

$$\begin{bmatrix} \varrho(F_1) \\ \varrho(G_1) \end{bmatrix} \equiv \begin{bmatrix} 0 & 1 \\ 1 & -1 \end{bmatrix} \begin{bmatrix} \varrho(F) \\ \varrho(G) \end{bmatrix} \pmod{1}. \quad (3.3)$$

This equation defines a hyperbolic map on the torus \mathbb{T}^2 , related to Arnold's cat map [8]. It has a dense set of periodic orbits, with homoclinic or heteroclinic connections between any two them. In particular, every point $\begin{bmatrix} 0 \\ m/n \end{bmatrix}$ lies on a periodic orbit. If m and n are coprime, then its period agrees with the fundamental period $\ell(n)$ of the Fibonacci sequence modulo n . To see why, multiply both rotation vectors in (3.3) by n , to get a congruence modulo n over the integers. Denoting by U the 2×2 matrix in (3.3), the condition for a period ℓ is $U^\ell \equiv \text{I}$ modulo n . A straightforward computation shows that this condition holds if and only if ℓ is a period of the Fibonacci sequence modulo n . The smallest such integer $\ell > 0$ is known as the Pisano period $\ell(n)$. The two periods described earlier are $\ell(2) = 3$ and $\ell(4) = 6$. Periods $\ell(n)$ with odd n are not expected to occur in the AM model, due to a symmetry that implies $\varrho(E) + \varrho(-E) \equiv 1/2$ modulo 1.

For even n , the period $\ell(n)$ is a multiple of 3. Thus, we restrict our analysis to iterates \mathfrak{R}^ℓ with ℓ a multiple of 3. Notice that $\mathfrak{R}^\ell(P)$ can be obtained by first iterating $(F, G) \mapsto (G, FG^{-1})$ ℓ times, and then conjugating the resulting maps with a scaling

$$\Lambda_\ell(x, y) = (\alpha_*^\ell x, S^\ell e^{\sigma_\ell S} y), \quad (3.4)$$

where $\sigma_\ell = \sigma_\ell(P)$ is determined by a suitable normalization condition.

The following result is a slight extension of Theorem 1.1 in [23].

Theorem 3.1. *\mathfrak{R}^3 has a reversible fixed point $P_* = (F_*, G_*)$ with F_* and G_* commuting. P_* is not a fixed point of \mathfrak{R} . The matrix parts of F_* and G_* are non-constant and extend to entire analytic functions. The scaling exponent $\sigma_* = \sigma_3(P_*)$ is positive and satisfies the bound $|\sigma_* - c_3| < 10^{-443}$, where $c_3 = 1/2 \cosh^{-1}(\alpha_*^{-1})$.*

We conjecture that $\sigma_* = c_3$ and note that the squared y -scaling factors $e^{\pm 2c_3}$ are the real roots of the polynomial $\mathcal{Q}_3(z) = z^4 - 2z^3 - 2z^2 - 2z + 1$.

The following theorem is proved in [24].

Theorem 3.2. \mathfrak{R}^6 has a reversible fixed point $P_* = (F_*, G_*)$ with F_* and G_* commuting. P_* is not a fixed point of \mathfrak{R}^k for any positive $k < 6$. The matrix parts of F_* and G_* are non-constant and extend to entire analytic functions. The scaling exponent $\sigma_* = \sigma_6(P_*)$ is positive and satisfies the bound $|\sigma_* - c_6| < 10^{-431}$, where $c_6 = 1/2 \cosh^{-1}(\alpha_*^{-3})$.

We conjecture that $\sigma_* = c_6$ and note that $e^{\pm 2c_6}$ are the real roots of the polynomial $\mathcal{Q}_6(z) = z^4 - 8z^3 - 2z^2 - 8z + 1$.

The fixed point P_* described in Theorem 3.1 (Theorem 3.2) can be associated with the Pisano period $\ell = \ell(n)$ for $n = 2$ ($n = 4$). Numerically, P_* attracts the self-dual AM pair with energy E_ℓ under iteration of \mathfrak{R}^ℓ . In addition, we have numerical evidence for the existence of analogous fixed points for $n = 6$ and $n = 8$. The corresponding rotation number is $\varrho(G) = 1/n$ in all cases considered. The periods for $n = 6, 8$ are $\ell(n) = 24, 12$, and the corresponding energy values are $E_{12} = 1.990 \dots$ and $E_{24} = 1.888 \dots$, respectively. Our computations for $n = 8$ were carried out at sufficient accuracy to predict a scaling exponent $c_{12} = 1/2 \cosh^{-1}(\alpha^{-6})$. This was motivated by the observation that $c_6 = 2c_3$. A similar relation for c_{12} seems excluded.

Remark 1. For convenience we have labeled periodic orbits by their fundamental period ℓ . However, the torus map (3.3) can have several periodic orbits with fundamental period $\ell(n)$. They arise from Fibonacci integer sequences modulo n that do not include a consecutive pair $(0, 1)$. Furthermore, there could be more than one (or no) periodic orbit of \mathfrak{R} for some periodic orbits of the map (3.3).

Theorem 3.1 is proved by first solving the fixed point problem for the transformation

$$\mathfrak{R}_3(F, G) = (\Lambda_3^{-1} G F^{-1} G \Lambda_3, \Lambda_3^{-1} G^{-1} F G^{-1} F G^{-1} \Lambda_3), \quad (3.5)$$

which is obtained from \mathfrak{R}^3 by a “palindromic” re-arrangement of the factors $F^{\pm 1}$ and $G^{\pm 1}$. This transformation has the advantage that reversible pairs are mapped to reversible pairs, even if the component maps do not commute. After establishing the existence of a fixed point P_* for \mathfrak{R}_3 , we prove that its components F_* and G_* commute. An analogous approach is used in our proof of Theorem 3.2.

We note that, due to the scaling $x \mapsto \alpha_* x$ involved, the analysis can be carried out on a bounded domain in \mathbb{C} . Entire analyticity of the matrix functions $B_* = \text{mat } F_*$ and $A_* = \text{mat } G_*$ follows by iterating the fixed point equation and using that $x \mapsto \alpha_* x$ is analyticity improving. The same argument shows that A_* and B_* are exponentially bounded on all of \mathbb{C} . More specific bounds can be obtained by using information on the Lyapunov exponent of maps that are attracted to P_* under renormalization. Based on an explicit expression [21] for the Lyapunov exponent of complex-translated AM maps, we expect that $\log \|B_*(x)\|$ and $\log \|A_*(\alpha_* x)\|$ grow like $2\pi 5^{-1/2}|x|$ in the imaginary direction. This is consistent with the decay rate of the Taylor coefficient that we find numerically in the cases $\ell = 3$ and $\ell = 6$.

4. Scaling and universality

In both cases ($\ell = 3$ and $\ell = 6$) our analysis requires as input an approximate fixed point of \mathfrak{R}^ℓ . Such a pair $P_{k\ell}$ is obtained numerically by starting with the self-dual AM pair P with energy E_ℓ and computing $P_{k\ell} = \mathfrak{R}^{k\ell}(P)$ for some large k . The fact that this procedure works suggests that P is attracted to our fixed point P_* under the iteration of \mathfrak{R}^ℓ . If we assume that this is the case, then it is possible to relate asymptotic properties of P to local properties of the transformation \mathfrak{R} near the orbit of P_* . Since \mathfrak{R} defines a dynamical system on a space of pairs, the same applies to other families in the domain of \mathfrak{R} .

Consider e.g. a Schrödinger operator \mathcal{H}^{α_*} and the associated map $G = (\alpha_*, A)$. Let $P = ((1, I), G)$ and $(F_n, G_n) = \mathfrak{R}^n(P)$. Then $G_n = \Lambda_n^{-1} G^{q_n} \Lambda_n$, where q_n is the $n + 1^{\text{st}}$ Fibonacci number. The matrix part of G^{q_n} is related to the matrix part A_n of G_n via

$$(\text{mat } G^{q_n})(\alpha_*^n x) = e^{\sigma_n S} S^n A_n(x) S^n e^{-\sigma_n S}. \quad (4.1)$$

If the sequence $k \mapsto P_{k\ell}$ converges to a fixed point P_* of \mathfrak{R}^ℓ , then $\sigma_{k\ell} \sim k\sigma_*$ for large k , where σ_* is the scaling exponent associated with P_* . This shows that the scaling factors e^{σ_*} given in Theorems 3.1 and 3.2 describe the asymptotic behavior of generalized eigenfunctions of \mathcal{H}^{α_*} with the proper rotation numbers. A precise argument along these lines is given in [23], as well as a graph of the generalized eigenfunction for the self-dual AM Hamiltonian for energy E_3 .

Concerning proper rotation numbers, we note that, while the periodic orbits of the map (3.3) are pairs with rational components, their stable manifolds include mostly irrational pairs. In particular, all pairs with $\varrho(F) = 0$ and $2\varrho(G) \in \mathbb{Z}[\alpha_*]$ are attracted to rational periodic orbits. Numerically, we find e.g. that the self-dual AM pair with $2\varrho(G) = 1 - \alpha_*$ is attracted under iteration of \mathfrak{R} to the 3-periodic orbit described in Theorem 3.1. The corresponding energy is $E = 1.874\dots$

Other universal quantities are associated with the eigenvalues of modulus ≥ 1 of the derivative of \mathfrak{R}^ℓ at a fixed point P_* . These eigenvalues have been determined numerically for the fixed points described in Theorems 3.1 and 3.2. In both cases, \mathfrak{R}^ℓ appears to be hyperbolic, with exactly two eigenvalues of modulus ≥ 1 . It seems likely that the same is true much more generally. In some sense, the “universality class” is governed by the two-parameter¹ AM model. To be more precise about hyperbolicity: We restrict \mathfrak{R}^ℓ to a codimension 1 manifold that includes all commuting pairs in the space being considered. Without this restriction, $D\mathfrak{R}^\ell(P_*)$ has a simple eigenvalue $(-1)^\ell$ that is associated with a non-commuting perturbation of P_* .

Two scaling phenomena that are governed by the largest eigenvalue μ_1 are described by (2.5). This eigenvalue determines the ℓ -step asymptotic scaling of the Hofstadter butterfly at (α_*, E_ℓ) in the energy direction. One of the assumptions here is that the AM family intersects the stable manifold of \mathfrak{R}^ℓ transversally; or equivalently, that this family converges to the unstable manifold of P_* under the iteration of \mathfrak{R}^ℓ and proper rescaling. To be more precise, let μ_2 be the second largest eigenvalue of $D\mathfrak{R}^\ell(P_*)$, and define $\mu s = (\mu_1 s_1, \mu_2 s_s)$

¹ We are not counting here the parameter α ; any scaling in the α direction is trivial and determined solely by arithmetic.

for all $s = (s_1, s_2)$ in \mathbb{R}^2 . For s near zero, denote by $P(s)$ the AM pair for $E = E_\ell + s_1$ and $\lambda = 1 + s_2$. Then the family $s \mapsto \mathfrak{R}^{k\ell}(P(\mu^{-k}s))$ is assumed to converge to a parametrization of the local unstable manifold of \mathfrak{R}^ℓ at P_* as k tends to infinity. We note that the diagonal nature of the parameter-scaling μ is specific to the AM family.

Consider e.g. the one-parameter family obtained by setting $s_2 = 0$. Assuming that the Lyapunov exponents and rotation numbers have limits as well, a straightforward computation yields the behavior (2.5) for positive $\epsilon = |s_1|$ close to zero.

Next, consider the one-parameter family obtained by setting $s_1 = 0$. Let $s_2 > 0$, and denote by $G(s_2)$ the second component of the pair $P(s)$. In this case, we already know that $L(G(s_2)) = \log(1 + s_2)$. So the assumptions made above yield a prediction for the eigenvalue μ_2 . Notice that, up to a conjugacy by $\Lambda_{k\ell}$, the second component of $\mathfrak{R}^{k\ell}(P(\mu^{-k}s))$ is the map $G(\mu_2^{-k}s_2)^{q_{k\ell}}$, where $q_n \simeq 5^{-1/2}\alpha_*^{-n-1}$ denotes the $n + 1^{\text{st}}$ Fibonacci number. Assuming that the Lyapunov exponent of $G(\mu_2^{-k}s_2)^{q_{k\ell}}$ converges to a finite nonzero value as $k \rightarrow \infty$, the above implies that $\mu_2 = \alpha_*^{-\ell}$. This value of μ_2 is indeed observed numerically, for the two periods $\ell(2) = 3$ and $\ell(4) = 6$.

We have also computed the first 12 contracting eigenvalues of $\mathcal{L} = D\mathfrak{R}_3^{\ell/3}(P_*)$. Numerically, the fifth largest (in modulus) eigenvalue μ_5 is a real root of the polynomial \mathcal{P}_ℓ , related to largest eigenvalue μ_1 as described after (1.3). For these real roots μ of \mathcal{P}_ℓ , one also finds that $x = \mu^{1/3}$ satisfies $x^4 - 3x^3 - x - 1 = 0$ in the case $\ell = 3$, while $x = \mu^{1/2}$ satisfies $x^4 - 14x^3 - 2x - 1 = 0$ in the case $\ell = 6$. The remaining eigenvalues of \mathcal{L} appear to be (real and) of the form $(\pm\alpha_*)^{k\ell}$, $(\pm\alpha_*)^{k\ell}e^{2c_\ell}$, or $(\pm\alpha_*)^{k\ell}e^{-2c_\ell}$, for some positive integer k . Both signs appear, if we count multiplicities in the case $\ell = 6$. For at least one choice of the sign, the eigenvector is generated by a coordinate transformation or corresponds to a non-commuting direction; see [23] for details on how to determine these eigenvectors. For the other values we do not have an explanation.

Acknowledgments. The work of S.K. is supported in part by the National Science Foundation EPSCoR RII Track-4 Award No. 1738834.

References

- [1] P.G. Harper, *Single band motion of conduction electrons in a uniform magnetic field*, Proc. Phys. Soc. Lond. A **68**, 874–892 (1955).
- [2] D.R. Hofstadter, *Energy levels and wave functions of Bloch electrons in rational and irrational magnetic fields*, Phys. Rev. B **14**, 2239–2249 (1976).
- [3] S. Aubry, G. André, *Analyticity breaking and Anderson localization in incommensurate lattices*, Ann. Israel Phys. Soc. **3**, 133–164 (1980).
- [4] J. Bellissard, B. Simon, *Cantor spectrum for the almost Mathieu equation*, J. Funct. Anal. **48**, 408–419 (1982).
- [5] D.J. Thouless, M. Kohmoto, M.P. Nightingale, M. den Nijs, *Quantized Hall conductance in a two-dimensional periodic potential*, Phys. Rev. Lett. **49**, 405–408 (1982).
- [6] R. Johnson, J. Moser, *The rotation number for almost periodic potentials*, Commun. Math. Phys. **84**, 403–438 (1982).
- [7] J. Avron, B. Simon, *Almost periodic Schrödinger operators. II. The integrated density of states*, Duke Math. J. **50**, 369–391 (1983).

- [8] F.J. Dyson, H. Falk, *Period of a discrete cat mapping*, Amer. Math. Monthly **99**, 603–614 (1992).
- [9] Y. Last, *A relation between a.c. spectrum of ergodic Jacobi matrices and the spectra of periodic approximants*, Commun. Math. Phys. **151**, 183–192 (1993).
- [10] Y. Last, *Zero measure spectrum for the almost Mathieu operator*, Comm. Math. Phys. **164**, 421–432 (1994).
- [12] A. Rüdinger, F. Piéchon, *Hofstadter rules and generalized dimensions of the spectrum of Harper’s equation*, J. Phys. A **30**, 117–128 (1997).
- [13] A.G. Abanov, J.C. Talstra, P.B. Wiegmann, *Hierarchical structure of Azbel-Hofstadter problem: strings and loose ends of Bethe ansatz*, Nuclear Physics B **525**, 571–596 (1998).
- [14] B.D. Mestel, A.H. Osbaldestin, B. Winn, *Golden mean renormalisation for the Harper equation: the strong coupling fixed point*, J. Math. Phys. **41**, 8304–8330 (2000).
- [15] D. Osadchy, J.E. Avron, *Hofstadter butterfly as quantum phase diagram*, J. Math. Phys. **42**, 5665–5671 (2001).
- [16] M.D. Choi, G.A. Elliott, N. Yui, *Gauss polynomials and the rotation algebra*, Invent. Math. **99**, 225–246 (2002).
- [17] J. Dalton, B.D. Mestel, *Renormalization for the Harper equation for quadratic irrationals*, J. Math. Phys. **44**, 4776–4783 (2003).
- [18] J. Puig, *Cantor spectrum for the almost Mathieu operator*, Commun. Math. Phys. **244**, 297–309 (2004).
- [19] M. Goldstein and W. Schlag, *Fine properties of the integrated density of states and a quantitative separation property of the Dirichlet eigenvalues*, Geom. Funct. Anal. **18**, 755–869 (2008).
- [20] A. Avila, S. Jitomirskaya, *The ten martini problem*, Ann. Math. **170**, 303–342 (2009).
- [21] A. Avila, *Global theory of one-frequency Schrödinger operators*, Acta Math. **215**, 1–54 (2015).
- [22] I.I. Satija, *A tale of two fractals: the Hofstadter butterfly and the integral Apollonian gaskets*, Eur. Phys. J. Spec. Top. **225**, 2533–2547 (2016).
- [23] H. Koch, *Golden mean renormalization for the almost Mathieu operator and related skew products*, Preprint 2019, mp_arc 19-45, arXiv:1907.06804 [math-ph].
- [24] H. Koch, S. Kocić, *Orbits under renormalization of skew-product maps over circle rotations*, In preparation.